ELECTROCHEMICAL STUDY OF THIENYL- AND FURYL-AZULENE-PYRIDINES AND FILM FORMATION

Alexandra OPRISANU[1], Ovidiu-Teodor MATICA[2],
Eleonora-Mihaela UNGUREANU[3]*, Mihaela CRISTEA[4], Liviu BIRZAN[5]

This work is devoted to the electrochemical characterization of two related azulene-pyridine compounds. The investigations were performed by cyclic voltammetry and differential pulse voltammetry. The main redox peaks for each compound were established, assessed, and compared. Modified electrodes based on these compounds were obtained by scanning the electrode potential to positive values or controlled potential electrolysis. Coverage of the surface was evidenced by ferrocene redox probe.

Keywords: azulene-pyridine compounds, cyclic voltammetry, differential pulse voltammetry

1. Introduction

The electrochemical oxidation of aromatic heterocyclic, benzenoid, or nonbenzenoid molecules frequently leads to the formation of an electrically conducting organic polymer films on the electrode surface [1-5]. These films typically have good adhesion and electrical contact to the electrode surface. Thin films, when supported by an electrode surface, can be electrochemically cycled between the oxidized, conducting state, and the neutral, insulating state. Thicker films can be produced in the oxidized, conducting state and can be peeled off from the electrode surface to yield free-standing, electrically conducting films. Because these films are in the oxidized state, they represent polymeric cations, whereby their overall charge balance is achieved by the incorporation of counteranions which stem from the electrolyte of the "electroplating" solution.

[1] Ph.D. student, Dept. of Inorganic Chemistry, Physical Chemistry and Electrochemistry, University POLITEHNICA of Bucharest, Romania, e-mail: oprisanualex@yahoo.com
[2] Ph.D. student, Dept. of Inorganic Chemistry, Physical Chemistry and Electrochemistry, University POLITEHNICA of Bucharest, Romania, e-mail: maticaovidiu@yahoo.co.uk
[3] * Emeritus Professor, Dept. of Inorganic Chemistry, Physical Chemistry and Electrochemistry, University POLITEHNICA of Bucharest, e-mail: em_ungureanu2000@yahoo.com
[4] Scientific Researcher, Institute of Organic Chemistry "C.D. Nenitzescu" of Romanian Academy, Bucharest, Romania, e-mail: mihcris2012@yahoo.ro
[5] Scientific Researcher, Institute of Organic Chemistry "C.D. Nenitzescu" of Romanian Academy, Bucharest, Romania

In this paper the electrochemical behaviour of the two azulene-pyridine compounds 2,6-bis((E)-2-(thiophen-2-yl)vinyl)-4-(4,6,8-trimethylazulen-1-yl)-pyridine (compound **1**) and 2,6-bis((E)-2-(furan-2-yl)vinyl)-4-(4,6,8-trimethylazulen-1-yl)-pyridine (compound **2**), was studied on a stationary electrode in acetonitrile containing tetra-butyl-ammonium perchlorate as supporting electrolyte.

The investigated pyridine compounds [6 - 8] with similar structures (Fig. 1), have two (thiophen-2-yl)vinyl- or (furan-2-yl)vinyl- substituents (for **1** and **2**, respectively) on the 4,6,8-trimethylazulene-pyridine skeleton. Un essential part of their structure is the 4,6,8-trimethylazulene, which can be polymerized by anodic oxidation [9 - 11]. **1** and **2** also contain a part of pyridine which is connected to 2 thiophene (**1**) or furane (**2**) rings, respectively, through vinyl fragments, insuring the extension of a conjugated structure of their molecules in comparison with similar previously investigated structures without vinyl [12, 13].

Cyclic and differential pulse voltammetry were employed to elucidate the electrode reactions of **1** and **2** using a glassy carbon electrode. The differential pulse and cyclic voltammetry data were examined in the light of the influence of the heteroatom electronegativity on oxidation and reduction proprieties.

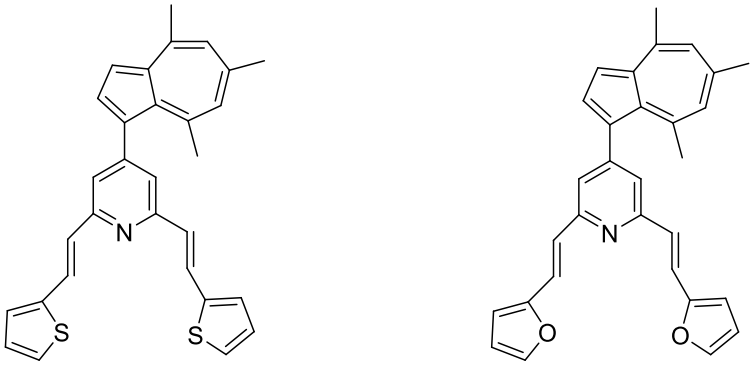

1 **2**

Fig.1. Structures of the investigated compounds

2. Experimental

Azulene-pyridine compounds **1** and **2** have been synthesized and characterized by physical chemical methods [6, 12]. Acetonitrile and tetrabutylammonium perchlorate (TBAP) from Fluka were used as received as solvent and supporting electrolyte.

The electrochemical experiments by cyclic voltammetry (CV) and differential pulse voltammetry (DPV) were carried out using a PGSTAT 12 AUTOLAB potentiostat in a three-compartment cell. The CV curves were

generally recorded at a scan rate of 0.1 Vs^{-1} or at various scan rates (0.1 - 1 Vs^{-1}) - when studying the influence of this parameter. DPV curves were recorded at 0.01 $V \cdot s^{-1}$ with a pulse height of 0.025 V and a step time of 0.2 s. The working electrode was a glassy carbon disk (having the diameter of 3 mm). The active surface was polished before each experiment with diamond paste (0.2 μm) and cleaned with acetonitrile. The Ag/10 mM $AgNO_3$ in 0.1 M TBAP, CH_3CN was used as reference electrode. The potential was finally referred to the potential of the ferrocene/ferricinium redox couple (Fc/Fc^+) which in our experimental conditions was +0.07V. A platinum wire was used as auxiliary electrode. The experiments were performed at the room temperature under argon atmosphere.

Chemically modified electrodes (CMEs) starting from **1** and **2** were prepared by scanning or controlled potential electrolysis (CPE) in millimolar solutions of each ligand in 0.1 M TBAP, CH_3CN. After preparation CMEs were cleaned with CH_3CN and transferred in ferrocene solution (1.5 mM) in 0.1 M TBAP, CH_3CN. The CV curves of ferrocene were recorded on bare electrode and on CMEs.

3. Results and Discussion

The anodic and cathodic curves in CV and DPV experiments were recorded individually, starting from the stationary potential. CV and DPV curves were collected for various concentrations (0 - 2mM for the investigated compounds) in 0.1 M tetrabutylammonium perchlorate (TBAP) solutions in acetonitrile (CH_3CN). The data from cyclic voltammetry experiments allowed to estimate the reversible (r), quasireversible (q) and irreversible (i) character of each peak.

*Study of **1***

The DPV curves obtained for different concentrations of **1** are presented in Fig. 2. Three anodic (1a - 3a) and three cathodic (1c - 3c) processes are noticed, denoted in the order in which they appear in the voltammograms. The CV curves for increasing concentrations of **1** are also shown in parallel with DPV curves in Fig. 2.

The influences of the potential scan range and scan rate on the CV curves obtained for the concentration of 2 mM are presented in Fig. 3. The data from Fig. 2 and 3 allows the possibility to establish the character of each process, as shown in Table 1 (reversible, quasi-reversible, or irreversible). Table 2 gives the values potential for the peaks at different concentrations from DPV corresponding to anodic and cathodic processes of compound **1**. The plot of anodic and cathodic peak currents is given in Fig. 4, and the equations of current dependencies on concentration i (c) are given in Table 3.

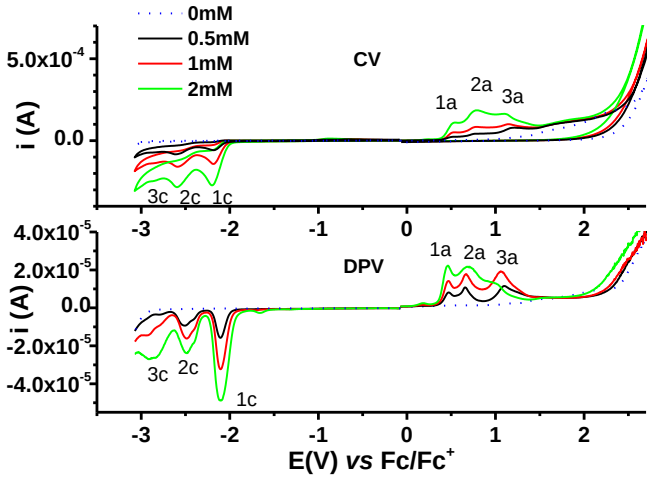

Fig. 2. CV and DPV curves (at 0.1 V/s) for different concentrations of **1** in 0.1M TBAP, CH_3CN on glassy carbon (3mm diameter)

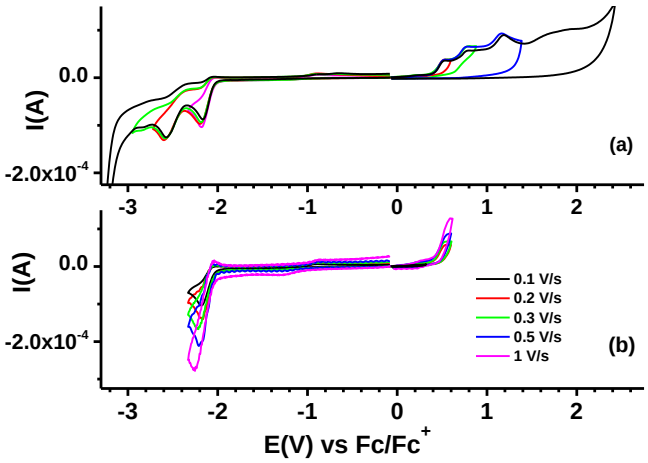

Fig. 3. CV curves at various scan domains at 0.1 Vs^{-1}, respectively(a) and at different scan rates: 0.1; 0.2; 0.3; 0.5; 1 Vs^{-1} in the domains of the peaks 1c and 1a (b) for **1** (2 mM) in 0.1M TBAP, CH_3CN

Table 1

Potentials (V) of the DPV and CV peaks and their assessment for 1

Symbol of the peak	Technique		Assesment
	DPV	CV*	
1c	-2.10	-2.18 **(r/q)**	Reduction of vinyl
2c	-2.50	-2.59 **(q)**	
3c	-2.92	-2.86 **(i)**	
1a	0.47	0.41 **(i)**	Oxidation of azulene
2a	0.67	0.77 **(q)**	Film formation
3a	1.09	1.18 **(i)**	

*r - reversible process; q - quasi-reversible process; i - irreversible process.

Table 2

Potential values of the peaks at different concentrations using DPV technique for anodic and cathodic processes of compound 1

c[mM]	E1a (V)	E2a (V)	E3a (V)	E1c (V)	E2c (V)	E3c (V)
0.5	0.46	0.66	1.09	-2.11	-2.51	-2.80
1	**0.46**	**0.67**	**1.06**	**-2.11**	**-2.49**	**-2.81**
2	0.45	0.69	1.02	-2.11	-2.49	-2.83

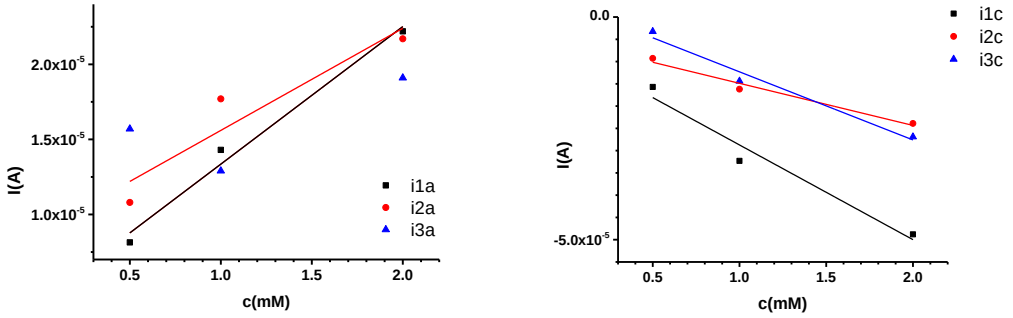

Fig. 4. Dependencies of anodic (A) and cathodic (B) peak currents on concentration of **1** from DPV experiments

Table 3

Equation of current intensity (A) values vs concentration of compound 1 (c, in mM) of the DPV peaks for anodic and cathodic processes

Peak	Equation of the peak current intensity	Correlation coefficient (R^2)
1a	4.19·E-6 +9.16·E-6·c	0.972
2a	8.8·E-6 + 6.8·E-6·c	0.774
3a	No linear correlation	-
1c	-7.45·E-6-2.13·E-5·c	0.927
2c	-5.43·E-6- 9.45·E-6·c	0.950
3c	2.99·E-6-1.53·E-5·c	0.951

It can be noticed that the concentration dependencies of the anodic peak currents 1a and 2a have different slopes resulting in an average of about 8·mA·$(M)^{-1}$, half value in respect to that for the cathodic peaks 15 ·mA·$(M)^{-1}$. These dependencies are useful for the assessment of concentrations of **1** using the DPV method. No linear correlation was found for 3a peak as this peak is involved in the film formation (Table 1). The peak potentials (Table 2) are independent on concentration of **1**.

*Study of **2***

The DPV curves obtained for different concentrations of **2** are presented in Fig. 5 (down). Two anodic (1a - 2a) and five cathodic (1c-5c) processes are

noticed, denoted in the order in which they appear in the voltammograms. The CV curves for increasing concentrations of **2** are also shown up in Fig. 5.

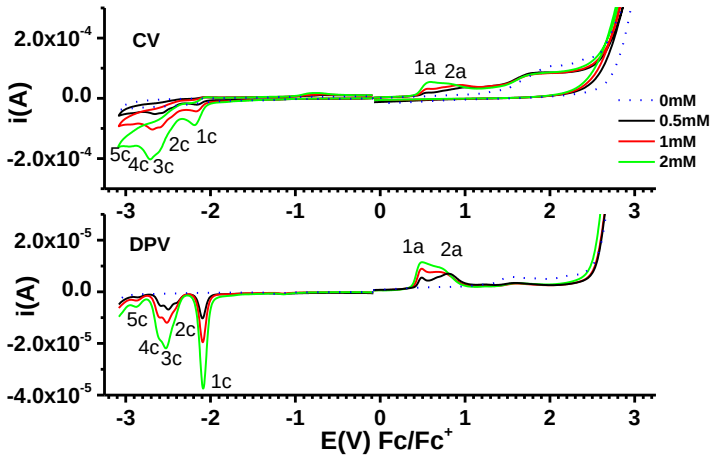

Fig 5. CV and DPV curves (at 0.1 Vs^{-1}) for different concentrations of **2** in 0.1M TBAP, CH_3CN, on glassy carbon (3 mm in diameter)

The influences of the potential range scanned and scan rate on the CV curves are presented in Fig. 6. The data from Figs. 5 and 6 allow establishing the character of each peak (Table 4).

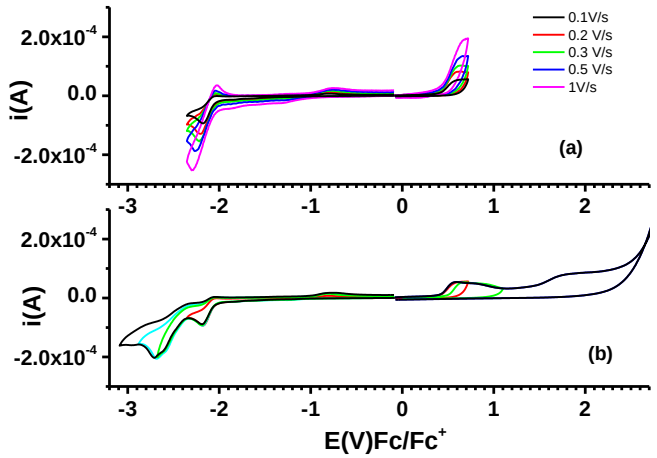

Fig. 6. CV curves at different scan rates in the domains of the peaks 1c and 1a, respectively, for [**2**] = 1.5 mM (a), and at various scan domains at 0.1 Vs^{-1} (b)

The obtained peaks for **2** were assessed as summarized in Table 4, where the main oxidation and reduction processes are included. Table 5 shows the

potential values of the peaks at different concentrations from DPV for anodic and cathodic processes of compound **2**.

Table 4

Potentials (V) of the DPV and CV peaks and their assessment for 2

Symbol of the peak	Technique		Assessment
	DPV	CV*	
1c	-2.09	-2.162**(r/q)**	Reduction of vinyl
2c	-2.411	-2.459	
3c	-2.495	-2.581**(i)**	
4c	-2.585	-2.664	
5c	- 2.865	-2.943	
1a	0.486	0.547	Oxidation of azulene
2a	0.814	0.998	Film formation

*r - reversible process; q - quasi-reversible process; i - irreversible process.

Table 5

Potential values of the peaks at different concentrations using DPV technique for anodic and cathodic processes of compound 2

c [mM]	E1a (V)	E2a (V)	E1c (V)	E2c (V)	E3c (V)	E4c (V)	E5c (V)
0.5	0.486	0.822	-2.095	-2.403	-2.495	-2.59	-2.865
1	**0.486**	**0.719**	**-2.091**	**-2.411**	**-2.51**	**-2.602**	**-2.868**
1.5	0.486	0.719	-2.084	-2.431	-2.52	-2.619	-2.868

Table 6

Equation of current intensity (A) values vs concentration of compound 2 (c, in mM) of the DPV peaks for anodic and cathodic processes

Peak	Equation of the peak current intensity	Correlation coefficient (R^2)
1a	2.9E-6+ 5.96E-6·c	0.987
2a	5.71E-6 + 2.53E-6·c	0.862
1c	4.75E-6 –2.696E-5·c	0.93
2c	-3.58E-7 –7.256E-6·c	0.905
3c	1.462E-6 –1.515E-5·c	0.937
4c	1.048E-6 –1.23E-5·c	0.957
5c	-2.76·E-7 –3.565E-6·c	0.886

It can be noticed that the concentration dependency of the anodic peak currents 1a and 2a is well correlated with concentration c with the slope of about 4 $mA\cdot(M)^{-1}$ while for the cathodic peaks 1c-5c the correlations are good, but their slopes are not the same (with a mean value of 13 $mA\cdot(M)^{-1}$). That for 1c (~27 $mA\cdot(M)^{-1}$) is four times higher than that for 2c, while 3c is double of that for 2c. These dependencies are useful to build calibration curves using the DPV method. The peak potentials (Table 5) are almost constant, being independent on concentration of **2**.

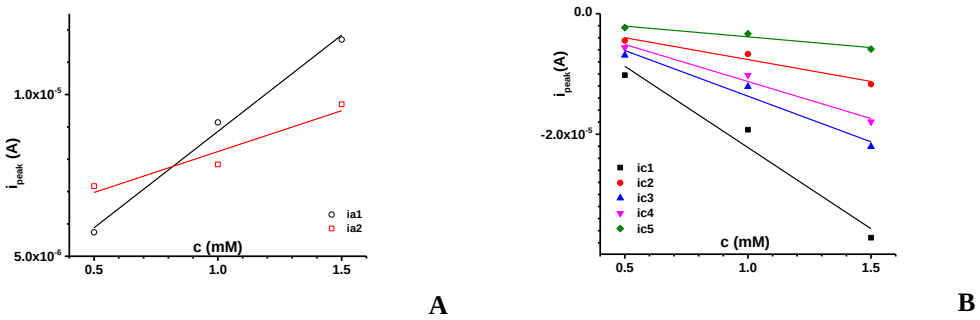

Fig. 7. Dependency of the peak curre of anodic (A) and cathodic (B) peak currents nts on concentration of **2** (expressed in mM)

The plot of anodic and cathodic peak currents is given in Fig. 7, and the equations of current dependencies on concentration i (c) are given in Table 6.

The concentration dependencies of the anodic peak currents are different resulting in an average of about 4 mA·(M)$^{-1}$, like those for cathodic peaks which is only in an average of about 13 mA·(M)$^{-1}$. These dependencies are useful for the assessment of concentrations of **2** using the DPV method.

*Comparison between electrochemical parameters of **1** and **2***

A detailed analysis of the peak's shapes and heights brought information about the redox behavior of these compounds. The structure of **1** and **2** presents a substituted azulene moiety connected (in position 4) to 2,6-bis((E)-2-(thiophen-2-yl)vinyl)- or 2,6-bis((E)-2-(furan-2-yl)vinyl)-pyridine. The alkyls substituents on azulene are all electron releasing substituents. Figures 2 and 5 allows the comparison between their curves. When examining the Table 2 and Table 5 for **1** and **2**, it could be seen that a1 process appears in the DPV of **1** at lower potential (0.47 V) than in **2** (0.486 V), while c1 process appears at a potential higher in absolute value (-2.11 V and -2.091 V, respectively). The obtained values are in agreement with the behavior of similar compounds without vinyl in their structure [13] being connected to the electronegativity of the heteroatom in these structures (S is less electronegative than O).

Film formation

The formation of a polyazulene film has been tried by successive scans in the domains of the anodic processes in millimolar solutions of each compound in CH_3CN + 0.1 M TBAP. The anodic and cathodic successive curves are given, for instance, for the compound **1** in the upper part of Fig. 8. The transfer of the CMEs obtained by scanning in ferrocene solution in CH_3CN + 0.1 M TBAP leads to CV

curves which are very different from those on bare electrode, as shown in Fig. 8 down.

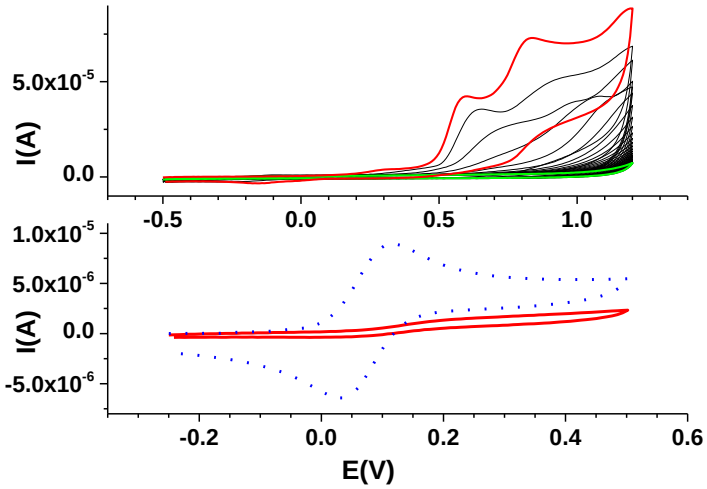

Fig 8. Successive CV anodic scans (0.1 V/s) on glassy carbon in 2mM solution of **1** in 0.1 M TBAP, CH_3CN (up), and the CV curves (0.1 V/s) in transfer solution (0.1M TBAP, CH_3CN) for the modified electrode obtained in this way by successive anodic CV scans (down) *vs* bare electrode (dotted line)

CMEs based on compound **1** were obtained also by CPE at anodic potentials. Their transfer in ferrocene solution led to perturbed CV signals as shown in Fig. 9.

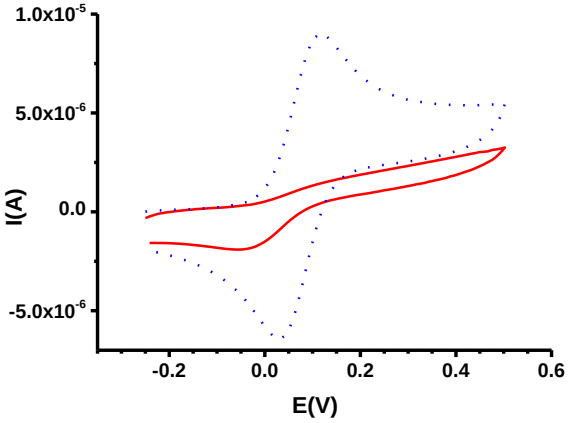

Fig 9. CV curves (0.1V/s) in transfer solution (0.1 M TBAP, CH_3CN) for the modified electrode obtained by CPE (2 mC) at 1.46 V in a solution of **1** (2 mM) in 0.1M TBAP, CH_3CN vs the bare electrode (dotted line)

For compound **2** the curves related to CMEs preparations by scanning and CPE are given in Fig. 10 and 11, respectively. Insulating polymeric films have been formed on the electrode surface also by CPE. Compound **2** showed a better potential for film formation than compound **1** as the film begins to form at lower potential, but a systematic study is necessary to reveal the differences between them.

In successive anodic scans, the oxidation peaks are shifted progressively to more positive values, indicating the electrode coverage with oxidation products in case of both azulene-pyridines **1** and **2** (Fig. 8 up and Fig. 10 up).

After the transfer in blank solution (0.1M TBAP, CH_3CN), the obtained modified electrode shows a stable behaviour in CV (curves not shown). To evaluate the deposits obtained either by scanning or CPE in each ligand solution, the corresponding CMEs were transferred in ferrocene solution in 0.1M TBAP, CH_3CN. Decreasing current intensity and shifting peak potentials for ferrocene indicate coating of the electrode surface with non-conductive films. The films grown by CPE have the same characteristics as those grown by scanning in the same synthesis solution. Fig. 9 shows the CV curve in transfer solution for the modified electrode obtained from **1** by CPE, while Fig. 11 that of the modified electrode obtained from **2**.

The formation of polyazulene film using compound **2** has been done in similar conditions as for compound **1**. The results are presented in Fig. 10 and Fig. 11.

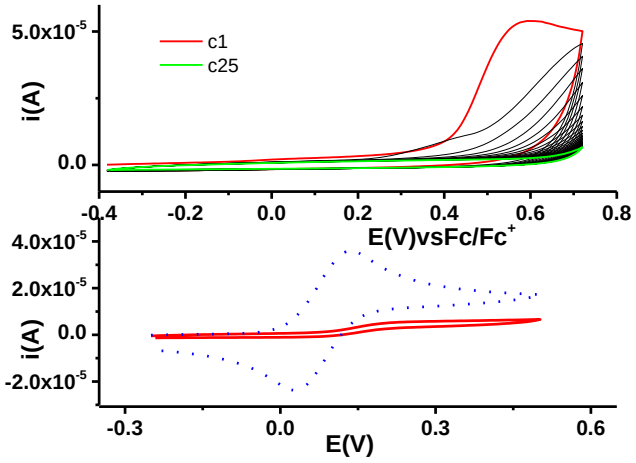

Fig.10. Successive CV anodic scans (0.1 V/s) on glassy carbon in 2mM solution of **2** in 0.1M TBAP, CH_3CN (up), and the CV curves (0.1 V/s) for the modified electrode obtained in this way by successive anodic CV scans in transfer solution (0.1M TBAP, CH_3CN) (down).

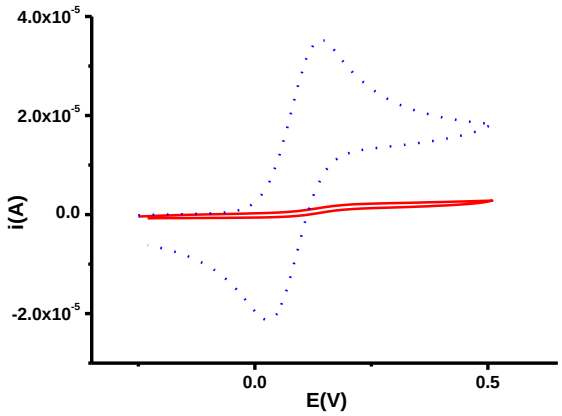

Fig 11. CV curves (0.1V/s) in transfer solution (0.1 M TBAP, CH_3CN) for the modified electrode obtained by CPE (0.8mC) at 0.95V in a solution of **2** (2 mM) in 0.1M TBAP, CH_3CN vs the bare electrode (dotted line)

4. Conclusions

This work explored the electrochemical properties of 2,6-bis((E)-2-(thiophen-2-yl)vinyl)-4-(4,6,8-trimethylazulen-1-yl)-pyridine (**1**) and 2,6-bis((E)-2-(furan-2-yl)vinyl)-4-(4,6,8-trimethylazulen-1-yl)-pyridine (**2**). The peak potential values and, therefore, the order in reduction or oxidation processes of compounds 1 and 2 are in agreement with the electronegativity of heteroatoms from their structure. Compound **1** is oxidized easier than compound **2**, and it is reduced harder.

Insulating polymeric films have been formed for both compounds on the electrode surface as proven by ferrocene redox probe. Although both show good potential for film formation, compound **2** presents a higher potentiality as the film begins to form at lower potentials. However, in view of further application as sensors, the direct tests of analytical samples will be the final response regarding their efficiency.

R E F E R E N C E S

[1]. *A.F. Diaz, K.K. Kanazawa, G.P. Gardini*, Electrochemical polymerization of pyrrole, J. Chem. Soc. Chem., **Chemical Communications**, 1979, pp. 635-636

[2]. *A.F. Diaz*, Electrochemical preparation and characterization of conducting polymers, Chemica Scripta, vol. **17**, 1981, pp. 145- 148

[3]. *G. Tourillon, F. Garnier*, New electrochemically generated organic conducting polymers, Journal of Electroanalytical Chemistry and Interfacial Electrochemistry, vol. **135**, 1982, pp. 173-178

[4]. *R.J. Waltman, A.F. Diaz, J. Bargon*, Substituent effects in the electropolymerization of aromatic heterocyclic compounds, The Journal of Physical Chemistry, *v*ol. **88**, 1984, pp. 4343-4346

[5]. *J. Bargon, S. Mohmand, R.J. Waltman*, Electrochemical synthesis of electrically conducting polymers from aromatic compounds, IBM Journal of Research and Development, vol. **27**, 1983, pp. 330-331

[6]. *A.C. Razus, S. Nica, L. Cristian, M. Raicopol, L. Birzan, A.E. Dragu*, Synthesis and physico-chemical properties of highly conjugated azo-aromatic systems. 4-(azulen-1-yl)-pyridines with mono- and bis azo-aromatic moieties at C3-position of azulene, Dye. Pigm., vol. **91**, 2011, pp. 55–61

[7]. *H. Xin, J. Li, R.Q. Lu, X. Gao, T.M. Swager*, Azulene–Pyridine-Fused Heteroaromatics, J. Am. Chem. Soc., vol. **142**, 2020, pp. 13598–13605

[8]. *A.C. Razus, L. Birzan, M. Cristea, E.A. Dragu, A. Hanganu*, Azulen-1-yl diazenes substituted at C-3 with phenyl-chalcogene moieties: dye synthesis, product characterization and properties, Monatshefte für Chemie-Chemical Monthly, vol. **142**, 2011, pp. 1271-1282.

[9]. *I.G. Lazar, E. Diacu, G.-L. Arnold, E.-M. Ungureanu, G.-O. Buica, L. Birzan*, Synthesis and characterization of poly(azulene-thiophene vinyl pyrylium) salt, Bulgarian Chemical Communications, Special Issue C, vol. **49**, 2017, pp. 227 – 232

[10]. *I.-G. Lazar, E. Diacu, E.-M. Ungureanu, G.-O. Buica, L. Bîrzan, G.-L. Arnold*, Modified electrodes based 2,6-bis((e)-2-(thiophen-2-yl)-4-(4,6,8-trimethylaazulen-1-yl) pyridine for heavy metals sensing, UPB Scientific Bulletin, Series B: Chemistry and Materials Science, 2017, Vol. **79** (3), pp. 23-36

[11]. *I.-G. Lazar, E. Diacu, G.-O. Buica, E.-M. Ungureanu, G.-L. Arnold, L. Birzan*, The heavy metals sensing based on 2,6-bis(-2-(thiophen-3-yl)vinyl)-4-(4,6,8-trimethylazulen-1-yl)pyrylium modified electrodes, Rev. de Chimie, vol. **68** (11), 2017 , pp. 2509-2513

[12]. *A.C. Razus, L. Birzan, C. Pavel, O. Lehadus, A. Corbu, F. Chiraleu, C. Enache*, Azulene--substituted pyridines and pyridinium salts. Synthesis and structure. 1. Azulene-substituted pyridines, J. Heterocycl. Chem., vol. **44**, 2007, pp. 245-250

[13]. *E.M. Ungureanu, G.O. Buica, A.C. Razus, L. Birzan, R. Weisz, M.R. Bujduveanu*, Electrochemical study on 4-(azulen-1-yl)-2, 6-bis (2-furyl)-nd 4-(azulen-1-yl)-2, 6-bis (2-thienyl)-pyridines, Rev. Chim, vol **63**, 2012, pp. 27–33